

Comparative study of Powder X-Ray Diffraction Analyses of Titanium Dioxide (TiO₂) Nanoparticles Synthesized by the Sol-Gel Method

Khyati Mody^a, I B Patel^b

Department of Physics, Veer Narmad South Gujarat University, Surat-395007, Gujarat, India.

^a kmody1997@gmail.com

^b ibpatel@vnsgu.ac.in

Abstract

This study presents a comparative analysis of Powder X-ray Diffraction (XRD) data of various Titanium Dioxide (TiO₂) nanoparticle samples synthesized via the Sol-Gel method using Titanium (IV) isopropoxide as a precursor. Titanium Dioxide, known for its chemical inertness and environmental friendliness, is widely utilized in industries as a pigment and exists in three crystalline phases: anatase, rutile, and brookite. XRD analysis revealed that the synthesized nanoparticles exhibit pure anatase and anatase-rutile mixed phases. The particle sizes, ranging in nanometres, were influenced by varying precursor ratios and calcination temperatures. Additionally, this research evaluates critical characteristics such as specific surface area, dislocation density, and morphology index, providing insights into the structural and physical properties of the prepared nanoparticles.

Keywords: Titanium Dioxide (TiO₂) nanoparticles, Sol-Gel Method, X-ray Diffraction (XRD), Anatase Phase, Dislocation Density, Morphology Index, Specific Surface Area.

Received 27 January 2025; First Review 21 February 2025; Accepted 06 March 2025

* Address of correspondence

Khyati Mody
Department of Physics, Veer Narmad South
Gujarat University, Surat-395007, Gujarat, India.

Email: kmody1997@gmail.com

How to cite this article

Khyati Mody, I B Patel, Comparative study of Powder X-Ray Diffraction Analyses of Titanium Dioxide (TiO₂) Nanoparticles Synthesized by the Sol-Gel Method, J. Cond. Matt. 2025; 03 (01): 30-35

Available from:
<https://doi.org/10.61343/jcm.v3i01.71>



Introduction

Titanium Dioxide (TiO₂) which is also defined as titania is one of the most versatile and widely studied materials in modern science and technology. Known for its exceptional chemical inertness, thermal stability, and environmental friendliness, TiO₂ is a naturally occurring oxide of titanium. It exists in three primary crystalline forms: anatase, rutile, and brookite, each possessing unique physical and chemical properties. Among these, the anatase and rutile phases are of particular interest due to their remarkable photocatalytic performance and optical characteristics. The anatase phase is known for its high reactivity and is often used in photocatalysis, while the rutile phase exhibits better thermal and structural stability.

Due to its non-toxic nature and strong UV light absorption, TiO₂ has found widespread applications across various industries. In the pigment industry, it serves as an essential component for paints, coatings, and plastics, providing superior opacity and brightness. In the cosmetics sector, it is used in sunscreens and skincare products to protect

against harmful UV radiation. Titanium Dioxide used in the pigment industry can also be defined as titanium white or pigment white. Furthermore, TiO₂ has gained significant attention in environmental applications, such as air purification, water treatment, and self-cleaning surfaces, owing to its photocatalytic properties that enable the breakdown of organic pollutants.

In recent years, TiO₂ has emerged as a key material in renewable energy technologies. It is widely used in dye-sensitized solar cells (DSSCs) and as a photocatalyst for hydrogen production through water splitting. Its ability to function as a photocatalyst under UV light has also led to innovations in energy-efficient coatings and anti-bacterial surfaces. Moreover, its abundance in nature, low cost, and ease of synthesis have contributed to its growing importance in industrial and research domains.

Extensive studies are being conducted to further enhance the efficiency and functionality of TiO₂, particularly by tailoring its properties through methods such as doping, surface modification, and nano-structuring. These

advancements aim to optimize its performance for specific applications and explore its potential in emerging fields like biomedical devices, sensors, and advanced energy storage systems.

Overall, the versatility, affordability, and eco-friendly nature of Titanium Dioxide make it an indispensable material in both traditional industries and cutting-edge technological advancements.

The Sol-Gel method is a cost-effective and versatile chemical route for synthesizing metal oxide (MO) nanoparticles, offering precise control over particle size and morphology. X-ray diffraction (XRD) is a fundamental tool for phase identification, lattice parameter determination, and crystallite size estimation. This study aims to compare the structural properties of TiO_2 nanoparticles synthesized via the Sol-Gel method under various conditions using XRD analysis.

Experimental Methods

Materials

Table 1: Materials used in the synthesis of TiO_2

Chemical Name	Chemical Structure
Titanium tetraisopropoxide (TTIP) [the titanium precursor]	$\text{Ti}\{\text{OCH}(\text{CH}_3)_2\}_4$
Acetic acid	CH_3COOH
Distilled water	H_2O

Methodology

The Sol-Gel method is a versatile chemical process widely used for synthesizing advanced materials, such as nanoparticles, thin films, and ceramics. It involves a transformation from a liquid solution (sol) into a solid network (gel) through hydrolysis and condensation reactions of metal alkoxides or inorganic salts. This technique allows precise control over material properties, including particle size, morphology, and composition.

One of the main benefits of the Sol-Gel method is its ability to synthesize materials at relatively low temperatures, which is an advantage over traditional high-temperature techniques. The process generally starts with the preparation of a precursor solution, typically using metal alkoxides like titanium (IV) isopropoxide. This solution undergoes hydrolysis and condensation, leading to the formation of a gel. Subsequent drying and calcination convert the gel into the desired crystalline phase with specific structural characteristics.

The Sol-Gel method is highly adaptable and can produce materials in various forms, such as powders, thin films, fibers, or monolithic structures. It is widely employed in applications like optical coatings, catalysts, sensors, and bioactive materials. The technique is especially valued for producing highly pure and homogeneous materials, essential for many advanced technologies.

In recent developments, the Sol-Gel process has become

increasingly popular for synthesizing metal oxide nanoparticles, including Titanium Dioxide (TiO_2). This method provides precise control over the structural and surface properties of nanoparticles, making it ideal for applications in photocatalysis, energy storage, and environmental cleanup. Its simplicity, cost-effectiveness, and scalability have made the Sol-Gel method a favored choice in both academic research and industrial manufacturing.

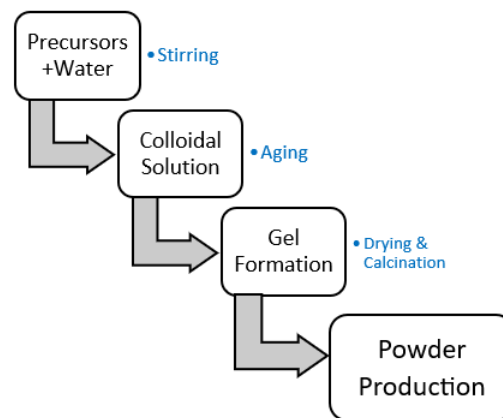


Figure1: The flowchart of Sol-gel synthesis.

The Sol-Gel process for Titanium Dioxide involved the hydrolysis and condensation of TTIP. The procedure was as follows:

1. Mix 20 ml of titanium isopropoxide with 40 ml of glacial acetic acid.
2. Stir the mixture using a magnetic stirrer until a homogeneous solution forms.
3. Gradually add 120 ml of deionized water to the solution, drop by drop, while stirring continuously for 2 hours to form the sol.
4. Place the solution in an oven set at 90°C and heat for about 12 hours to facilitate gel formation.
5. Pulverize and dry the gel at 200°C for 2 hours, resulting in the formation of a white powder.



Figure 2: Transformation of Sol to Gel.

I have carried out the experiment by changing different parameters like the precursor ratio, water amount and the calcination temperature by 200°C , 400°C and 500°C which is shown in a table form as follows:

Table 2: The change in the different parameters with the different samplings.

Sample	TTIP (ml)	Acetic Acid (ml)	Dist. Water (ml)	Temperature °C
S1	20	40	120	200
S2	30	40	120	200
S3	20	40	200	200
S4	20	40	120	400
S5	25	45	125	500

Results and Discussion

Characterization

X-Ray diffraction is basically one of the most useful powder analysis techniques used for the detailed study of nanomaterial's structural belongings for all the types of crystal clear, limpid, transparent, and composed of crystals. X-ray diffraction analysis can be used for the following aspects:

- **Crystallinity:** Can point out whether nanoparticles are crystalline or amorphous in nature.
- **Phase:** Can pick out the phase of polycrystalline materials and compounds.
- **Crystal orientation:** Can provide detailed data on the preferred crystal orientation of a material.
- **Grain size:** Can provide details on the average grain size of a material.
- **Strain:** Can provide information on the strain in a material.
- **Crystal defects:** Can supply the data on how the crystal defects are forming inside any material.

Principle of XRD: It operates on the principle of constructive interference, where monochromatic X-rays interact with the periodic lattice planes of a crystal. When an X-ray beam strikes a crystalline material, diffraction takes place in accordance with Bragg's Law.

Steps in XRD Analysis of the Experiments-

1. Sample Preparation

Five different powder samples have been prepared using the methodology, packed in glass bottles keeping stored at the room temperature and then sent to the laboratory for the analysis.

Divergence Slit: A fixed divergence slit with a size of 0.3599° was used.

Specimen Details: The specimen length was 10 mm, and measurement was conducted at 25°C . **Anode Material:** Copper (Cu) was used as the anode material with $(\lambda)=1.5406 \text{ \AA}$.

2. Data Collection

The scan was performed in Gonio mode, covering a 2θ range from 10.0066° to 89.9956° with a step size of 0.013° and a step time of 18.87 seconds. The scan type was continuous. The XRD pattern is recorded as intensity versus the diffraction angle (2θ) for each sample.

3. Analysis

The peaks in the XRD pattern are matched with reference patterns to identify phases.

4. Calculations

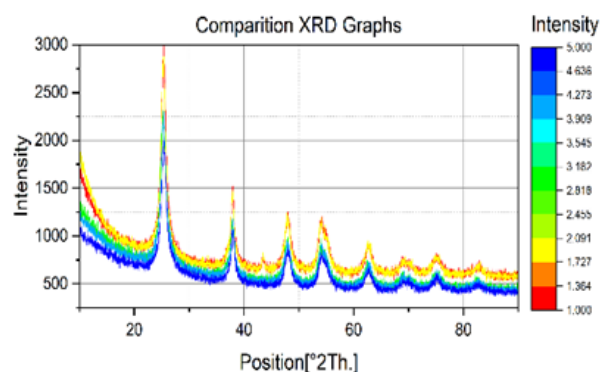
Additional parameters have been calculated from the peak width and position. The result of which confirmed the nanosize of TiO_2 .

5. Comparison

Five different samples undergo the calculations and the detailed datasheet was prepared for the comparison.

Results

The comparison graph of all the TiO_2 nanoparticle samples is shown here in the below figure3. This shows the decrease in the peak intensity confirming the anatase phase.

**Figure 3:** The peak intensity comparison of nanosized TiO_2 .

X-Ray Diffraction analysis is a widely used technique for assessing the crystallinity of synthesized nanoparticles (NPs). The height of the peaks shown in the XRD graph for all the different samples indicate whether the nanoparticles are crystalline or amorphous.

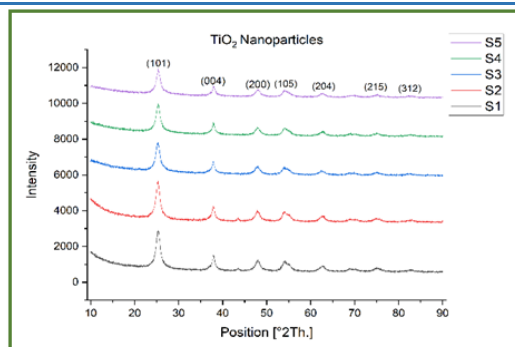


Figure 4: X-Ray Diffraction patterns of TiO₂ samples

Figure above shows the X-Ray Diffraction patterns of five different nanosized TiO₂ samples labelled as S1, S2, S3, S4 and S5 with the varying conditions given in the table2 above. The experimental XRD pattern agrees with the JCPDS card no. 21-1272 (anatase TiO₂) and the XRD pattern of TiO₂ nanoparticles other literature. High intensity peaks at around 25 °C and 37 °C strongly confirms the presence of Anatase phase of TiO₂ nanoparticles. The crystallite size of these particles can be measured using Debye–Scherrer’s formula:

$$D = \frac{0.94\lambda}{\beta \cos\theta}$$

Where, 0.94 is the shape factor, λ is the wavelength of the X-ray radiation for Cu K α , and β is the line width at half-maximum height. The position with the corresponding FWHM for all five samples is given in the below graph.

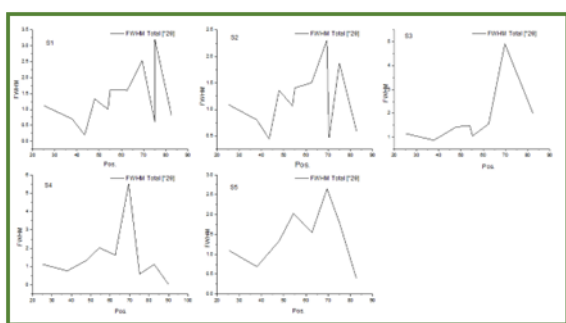


Figure 5: The FWHM versus Position graph of nanosized TiO₂.

The crystalline size with the corresponding FWHM for all five samples is given in the below table by using the equation given above:

Table 3: The change in the crystalline size by varying conditions for nanosized TiO₂.

Sample Name	FWHM (radian)	Crystalline size	Pos. [°2θ]
S1	0.01219	12.358	37.9004
S2	0.01402	10.667	37.8612
S3	0.01529	9.780	37.8327
S4	0.01330	11.245	37.9026
S5	0.01205	12.405	37.9466

The table summarizes the XRD analysis results for TiO₂ samples (S1 to S5), showing their Full Width at Half Maximum (FWHM), crystalline size, and peak positions at specific 2 θ angles. The FWHM values range from 0.01205 to 0.01529 radians, corresponding to crystalline sizes between 9.780 nm and 12.405 nm. The 2 θ positions of the diffraction peaks vary slightly among the samples, falling between 37.8327° and 37.9466°. This data reflects variations in the crystalline properties of the synthesized nanoparticles. This reflects that S3 with the maximum water part (200 ml) in it consists of the lowest particle size.

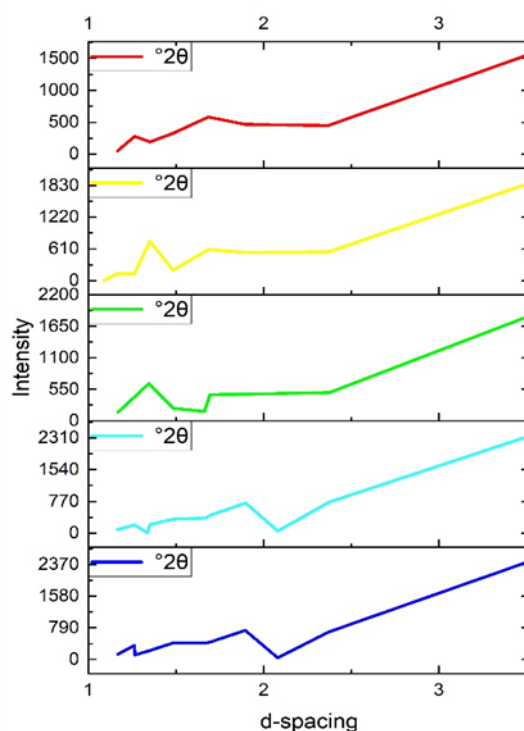


Figure 6: The comparison graph of TiO₂ nanoparticles for intensity versus d-spacing.

Significance of d-spacing

- Crystal Structure Identification:** The d-spacing values, combined with X-ray diffraction patterns, help identify the phases and structure of a material.
- Lattice Parameter Calculation:** It is used to calculate the lattice constants of a crystal system (e.g., cubic, tetragonal, hexagonal).
- Material Properties:** Changes in d-spacing can indicate lattice strain, defects, or distortions in the crystal structure.

Real-World Applications

Below are some emerging applications of TiO₂ nanoparticles in relation to the XRD findings:

Self-Cleaning Surfaces

TiO₂-coated surfaces exhibit superhydrophilicity and photocatalytic degradation of organic materials.

XRD analysis of crystallinity and phase composition can help optimize TiO₂ films for self-cleaning coatings used in windows, textiles, and solar panels.

Anti-Microbial and Bio-Medical Applications

TiO₂ nanoparticles show antibacterial properties under UV light, useful in hospital coatings, wound dressings, and implants.

XRD phase identification (anatase-dominant) can correlate with bioactivity and toxicity levels, ensuring safety in biomedical applications.

Hydrogen Production via Water Splitting

TiO₂ is a key material in photoelectrochemical (PEC) water splitting to generate hydrogen fuel.

XRD data on crystal phase, lattice strain, and oxygen vacancies can help optimize TiO₂ nanostructures for higher photocatalytic efficiency in hydrogen evolution.

Smart Windows and Electrochromic Devices

TiO₂ is used in smart glass technology that changes transparency based on external stimuli.

XRD studies can reveal structural stability, ensuring long-term performance in energy-efficient buildings and vehicles.

Conclusion

We have successfully synthesised TiO₂ nanoparticles by using the colloidal route of methodology said to be the Sol-Gel method in very safe and environment friendly atmosphere. By changing different parameters, we have seen the changes appearing in intensity, Full width at half maximum and the crystalline size. At the end we came to know that In the grown crystal the d-value is fingerprints of a specific sample which is determined by XRD. The shifting of plane d-spacing is due to the rearrangement of lattice positions. It is due to the doping of ions, atoms and impurities. Another thing which affects the d value is stress forces which is external forces.

Comparative analysis of the nanomaterials suggests:

- **Effect of Calcination Temperature:** Higher temperatures increased crystallinity but promoted the anatase-to-rutile phase transformation.
- **Effects of pH:** Alkaline conditions resulted in

mixed phases, while acidic conditions favored pure anatase.

- **Effect of Hydrous solution:** More hydrous solution decreases the crystallinity and hence particle size.

This comparative XRD analysis demonstrates that synthesis parameters such as calcination temperature and pH significantly influence the structural properties of TiO₂ nanoparticles. Optimal conditions for achieving high-purity anatase with small crystallite sizes were identified, providing a foundation for tailoring TiO₂ properties for specific applications. Future studies could explore doping effects and advanced characterization techniques to further enhance TiO₂ functionality.

Acknowledgement

The authors would be happy to thank the Sophisticated Analytical Instrumentation Facility, Punjab university, Chandigarh for providing XRD instrument to analyse the samples.

References

1. A. Fujishima, K. Honda, Electrochemical photolysis of water at a semiconductor electrode, *Nature* 238 (1972) 37–38.
<https://doi.org/10.1038/238037a0>.
2. C.H. Ao, S.C. Lee, Indoor air purification by photocatalyst TiO₂ immobilized on an activated carbon filter installed in an air cleaner, *Chem. Eng. Sci.* 60 (2005) 103–109.
<https://doi.org/10.1016/j.ces.2004.01.073>.
3. Y. Paz, Application of TiO₂ photocatalysis for air treatment: patents' overview, *Appl. Catal. B Environ.* 99 (2010) 448–460.
<https://doi.org/10.1016/j.apcatb.2010.05.011>.
4. M. Hussain, N. Russo, G. Saracco, Photocatalytic abatement of VOCs by novel optimized TiO₂ nanoparticles, *Chem. Eng. J.* 166 (2011) 138–149.
<https://doi.org/10.1016/j.cej.2010.10.040>.
5. S. Miar Alipour, D. Friedmann, J. Scott, R. Amal, TiO₂ /porous adsorbents: recent advances and novel applications, *J. Hazard. Mater.* 341 (2018) 404–423.
<https://doi.org/10.1016/j.jhazmat.2017.07.070>.
6. M. Landmann, E. Rauls, W.G. Schmidt, The electronic structure and optical response of rutile, anatase and brookite TiO₂, *J. Phys. Condens. Matter* 24 (2012) 195503.
<https://doi.org/10.1088/0953-8984/24/19/195503>.
7. B.L. Diffey, Sources and measurement of ultraviolet radiation, *Methods* 28 (2002) 4–13.
[https://doi.org/10.1016/S1046-2023\(02\)00204-9](https://doi.org/10.1016/S1046-2023(02)00204-9).

8. W.-J. Yin, S. Chen, J.-H. Yang, X.-G. Gong, Y. Yan, S.-H. Wei, Effective band gap narrowing of anatase TiO₂ by strain along a soft crystal direction, *Appl. Phys. Lett.* 96 (2010). <https://doi.org/10.1063/1.3430005> 221901.
9. R. Long, N.J. English, Band gap engineering of double- cation-impurity-doped anatase-titania for visible-light photocatalysts: a hybrid density functional theory approach, *Phys. Chem. Chem. Phys.* 13 (2011) 13698–13703. <https://doi.org/10.1039/C1CP21454C>.
10. S.G. Kumar, L.G. Devi, Review on modified TiO₂ photocatalysis under UV/Visible light: selected results and related mechanisms on interfacial charge carrier transfer dynamics, *J. Phys. Chem. A* 115 (2011) 13211–13241. <https://doi.org/10.1021/jp204364a>.
11. J. Godnjavec, J. Zabret, B. Znoj, S. Skale, N. Veronovski, P. Venturini, Investigation of surface modification of rutile TiO₂ nanoparticles with SiO₂/Al₂O₃ on the properties of polyacrylic composite coating, *Prog. Org. Coat.* 77 (2014) 47–52. <https://doi.org/10.1016/j.porgcoat.2013.08.001>.
12. S. Ke, X. Cheng, Q. Wang, Y. Wang, Z. Pan, Preparation of a photocatalytic TiO₂ / ZnTiO₃ coating on glazed ceramic tiles, *Ceram. Int.* 40 (2014) 8891–8895. <https://doi.org/10.1016/j.ceramint.2014.01.027>.
13. R. Phienluphon, K. Pinkaew, G. Yang, J. Li, Q. Wei, Y. Yoneyama, T. Vitidsant, N. Tsubaki, Designing core (Cu/ZnO/Al₂O₃)–shell (SAPO-11) zeolite capsule catalyst with a facile physical way for dimethyl ether direct synthesis from syngas, *Chem. Eng. J.* 270 (2015) 605–611. <https://doi.org/10.1016/j.cej.2015.02.071>.
14. Z. Li, Y. Hou, B. Ma, X. Wu, Z. Xing, K. Li, Super-hydrophilic porous TiO₂ -ZnO composite thin films without light irradiation, *Environ. Prog. Sustain. Energy* 35 (2016) 1121–1124. <https://doi.org/10.1002/ep.12308>.
15. Y. Yao, G. Li, S. Ciston, R.M. Lueptow, K.A. Gray, Photoreactive TiO₂ /carbon nanotube composites: synthesis and reactivity, *Environ. Sci. Technol.* 42 (2008) 4952–4957. <https://doi.org/10.1021/es800191n>.
16. Y.-J. Xu, Y. Zhuang, X. Fu, New insight for enhanced photocatalytic activity of TiO₂ by doping carbon nanotubes: a case study on degradation of benzene and methyl orange, *J. Phys. Chem. C* 114 (2010) 2669–2676. <https://doi.org/10.1021/jp909855p>.
17. Y. Liang, H. Wang, H. Sanchez Casalongue, Z. Chen, H. Dai, TiO₂ nanocrystals grown on graphene as advanced photocatalytic hybrid materials, *Nano Res.* 3 (2010) 701–705. <https://doi.org/10.1007/s12274-010-0033-5>.
18. Y. Zhang, Z.-R. Tang, X. Fu, Y.-J. Xu, TiO₂–graphene nanocomposites for gas-phase photocatalytic degradation of volatile aromatic pollutant: is TiO₂ –graphene truly different from other TiO₂ –carbon composite materials? *ACS Nano* 4 (2010) 7303–7314. <https://doi.org/10.1021/nn1024219>.
19. J. Liu, H. Bai, Y. Wang, Z. Liu, X. Zhang, D.D. Sun, Self-assembling TiO₂ nanorods on large graphene oxide sheets at a two-phase interface and their anti-recombination in photocatalytic applications, *Adv. Funct. Mater.* 20 (2010) 4175–4181. <https://doi.org/10.1002/adfm.201001391>.
20. K. Zhou, Y. Zhu, X. Yang, X. Jiang, C. Li, Preparation of graphene– TiO₂ composites with enhanced photocatalytic activity, *New J. Chem.* 35 (2011) 353–359. <https://doi.org/10.1039/C0NJ00623H>.
21. J. Auvinen, L. Wirtanen, The influence of photocatalytic interior paints on indoor air quality, *Atmos. Environ.* 42 (2008) 4101–4112. <https://doi.org/10.1016/j.atmosenv.2008.01.031>.
22. M. Nuño, R.J. Ball, C.R. Bowen, Study of solid/gas phase photocatalytic reactions by electron ionization mass spectrometry: study of photoreactions by mass spectrometry, *J. Mass Spectrom.* 49 (2014) 716–726. <https://doi.org/10.1002/jms.3396>.
23. M. Nuño, R.J. Ball, C.R. Bowen, R. Kurchania, G.D. Sharma, Photocatalytic activity of electrophoretically deposited (EPD) TiO₂ coatings, *J. Mater. Sci.* 50 (2015) 4822–4835. <https://doi.org/10.1007/s10853-015-9022-0>.
24. M. Nuño, G.L. Pesce, C.R. Bowen, P. Xenophontos, R.J. Ball, Environmental performance of nano-structured Ca(OH)₂/ TiO₂ photocatalytic coatings for buildings, *Build. Environ.* 92 (2015) 734–742. <https://doi.org/10.1016/j.buildenv.2015.05.028>.
25. P. Wolkoff, G.D. Nielsen, Organic compounds in indoor air-their relevance for perceived indoor air quality? *Atmos. Environ.* 35 (2001) 4407–4417. [https://doi.org/10.1016/S1352-2310\(01\)00244-8](https://doi.org/10.1016/S1352-2310(01)00244-8).